Report on Calculations Regarding ITM/ETM and Wide-Angle-Baffles (WAB) in the Cryostat

Simon Zeidler

NAOJ

Short Introduction and describtion

Regarding the scattering of light on the ITM/ETMs of KAGRA and the WAB (to be installed close to each test mass), calculations with the simulation tool “LightTools” have been done in order to reveal the most efficient design of WABs in terms of reduction of scattering, size, and costs of the baffles. The test masses are very crucial parts of KAGRA and thus sensible to even small amounts of scattering. But not last due to the limited space inside the cryostat, the installation of both WAB and payload with the test mass is a challange.

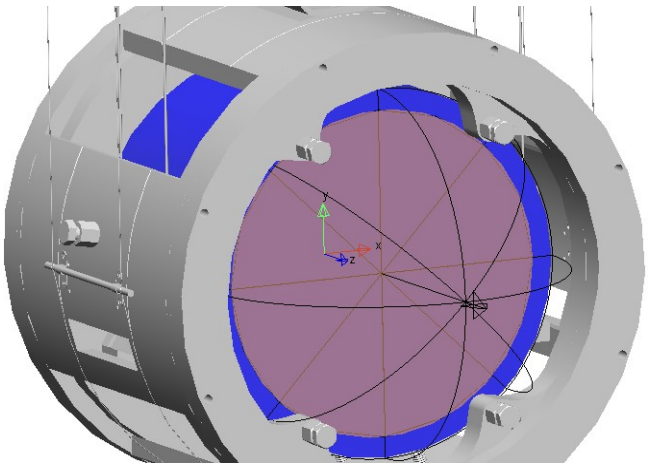

Figure 1: Model of the ITM with view on the front-side, facing the cavity. In blue the mirror itself is shown while the grey surroundings illustrate the recoil-mass with the respective wires. The high-lighted area on the mirror is the by the laser illuminated surface.

As a starting point for the simulations, the CAD-sketch of the ITM/ETM together with its recoil mass has been used and imported into “LightTools”. In Fig.1, a close view onto the front-side (the side facing the cavity) of the ITM/ETM is shown. The image has been taken with “LightTools” showing also the by the laser illuminated area on the mirror. This area actually worked as the basic light-source in the simulations as we are only interested in the light scattered by the mirror and a close-to-reality simulation with a separated laser source and a structured mirror-surface would not work properly as such tiny structures are impossible to be modeled by “LightTools”. The

distribution of the scattered light, has been calculated according to the multilayer scattering theory by Elson et al. (1981) and Bousquet et al. (1983), which is a first order vector perturbation theory to calculate the scattered power of coated surfaces by using the power-spectral density of the substrate's surface. The result for high-quality mirrors is a distribution of the scattered power of the Lorentz type with a distinct peak close to the specular reflection.
In addition to this "general" surface-scattering effect, so called point-defects will create a Lambertian-like scattering ($\rightarrow$Mie, white noise). After Hiro Yamamoto (LIGO) this additional influence can be approximated by $BRDF \approx 30/2\pi$ ppm. $BRDF$ means here "Bidirectional Reflection Distribution Function" and is the scattered power per unit solid-angle divided by the incoming power and the cosine of the latitude.

The back-scattered light (from structures close to the mirror) will recouple into the main beam if it hits the mirror where it is coming from. The probability of recoupling is assumed to be the same as or the original scattering on the surface. **(Should the point defects being excluded from the recoupling due to their tininess?)**. In Fig.2, such a map is presented as a superposition of the contributions from the mirror's roughness and the point defects.

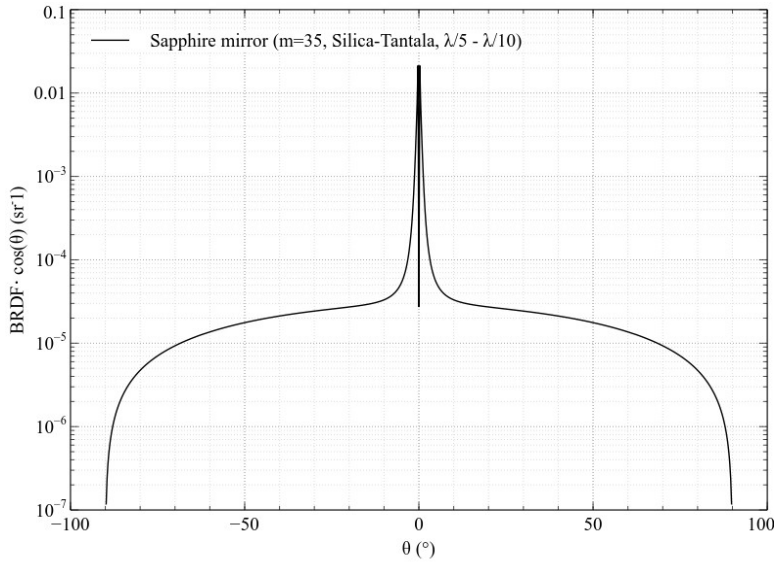

Figure 2: Distribution of the scattering probability as a function of the latitude along the plane of incidence for the sapphire mirror.

More specifically, the result of the mentioned scattering theory is a two-dimensional matrix giving information about the $BRDF$ as a function of both latitude θ and longitude ϕ relative to the mirror's surface. The graph in Fig.1 is only the cross section of the distribution map. Hence, there is no dependence on ϕ indicated.

The matrix has been implemented into the model by defining the angular probability distribution per steradian ($BRDF(\theta,\phi)\cdot\cos(\theta)$) of the scattered light.

The beam's intensity, coming to the mirror, however, is not homogeneously distributed but has a distribution of a Gaussian beam ($\sigma = 36\,mm$) as the laser in KAGRA would have. The overall

intensity of the scattered light has been set to 1W. It should be noted that the scattering has been set to zero for an interval of $\theta=[0, 9.29^{\circ}]$ in order to concentrate on the outcome of scattering at angles where hitting the inner shield, the assembly frame, or the recoil mass is guaranteed. The total scattering, however, is normalized to $TS=10^{-4}$.

The material of the recoil mass is Titanium and the simulations have been done by using experimentally data of the $BRDF$ of an unpolished Titanium-plate measured with our scatterometer at NAOJ.

To complete the simulations, also the assembly frame and the inner shield of the cryostat have been implemented into the model. All three (recoil mass, assembly frame, and inner shield) are the main objects which are receiving scattered light from the mirror and are close to it. The material of the assembly frame is mainly Aluminum while the inner shield consists of diamond-like carbon (DLC), an absorptive but shiny material.
However, in all these considerations, one should be aware of the influence of the scattering each coming from the opposite mirror in the cavity. Since the peak of scattering is strongest in the vicinity of the specular reflection (see Fig.2), the narrowest-angle scattering that reaches any edges of the inner shield, assembly frame, or recoil mass of the opposite mirror, may influence the recoupling budget stronger than any wide-angle scattering (Hiro Yamamoto, priv. comm.).
For that, simulations have to be done!

Influence of scattered light on the sensitivity of KAGRA

According to Flanagan and Thorne (1994), the (direction depending) irradiance of back-scattered light back to the mirrors is given by

$$\frac{\partial \delta P}{\partial A_M}=\frac{\partial P}{\partial \Omega_M}\delta\Omega\frac{\partial \rho}{\partial A_M} \quad ,$$

where $\frac{\partial P}{\partial \Omega_M}$ is the by the mirror scattered power and equals the mirror's scattering probability multiplied by the power of the incoming main beam, $\frac{\partial \rho_{bsc}}{\partial A_M}$ is the probability of backscattering to a surface unit of the mirror, and $\delta\Omega$ is the part of the solid angle in which the mirror's scattering happens. The part of the back-scattered light that is finally guided back into the main beam is calculated by multiplying above term with a certain cross section σ_{mb} , which is related to the mirror's scattering probability via

$$\sigma_{mb}=\lambda^2\frac{\partial \rho}{\partial \Omega_M} \quad ,$$

where λ is the wavelength of the scattered light (1064 nm in case of KAGRA).
The influence on the sensitivity of KAGRA is

$$\delta h^2(f)=\frac{\lambda^4}{(4\pi L)^2}\left(\frac{\partial \rho}{\partial \Omega_M}\right)^2\left(\frac{\partial \rho_{bsc}}{\partial A_M}\right)\widetilde{S}^2(f)\delta\Omega_M \quad .$$

With $\widetilde{S}(f)$ being the spectral density of the sine of the phase fluctuations which are carried by the

back-scattered light once they hit surfaces other than the mirror.

The main analyzing tool for the scattering simulations was the “LightTools” software. It is basically a ray-tracing program working with the Monte-Carlo calculation procedure. With this software it is possible to measure the irradiance (W/m^2) coming from a certain direction upon a defined surface (receiver).
As long as the incoming back-scattered light onto the mirror is more or less homogeneous, the mirror-surface itself can be taken as one receiver and the result of the simulations would give

$$\frac{dP_{rec}}{A_M\, d\Omega_{Mrec}} = \frac{P_{mb}}{A_M} \int_{\Omega_M} \int_{A_M} \frac{\partial \rho}{\partial \Omega_{Mscat}} \frac{\partial \rho_{bsc}}{\partial A_M}\, dA_M\, d\Omega_{Mscat},$$

the received power per unit steradiand of the mirror’s hemishpere divided by the surface area of the mirror. In terms of the sensitivity of KAGRA we would then have

$$h^2(f) = \frac{\lambda^4}{(4\pi L)^2} \frac{P_{rec}}{A_M P_{mb}} \left(\frac{\partial \rho_{rbs}}{\partial \Omega_M} \right) \widetilde{S}^2(f),$$

where ρ_{rbs} means the probability of recoupling of the back-scattered light into the main beam.
If the received power is strongly inhomogeneous, the mirror surface has to be split into several receivers so that the received power is again homogeneous for each receiver. The overall received power is then the sum of the results of each receiver.
(**I am not entirely sure but I guess there is a possibility in LightTools to take direction-depended intensity with a spatial luminescence detector. I have to proof that.**)

Results

Baffle design

I did the simulations with and without draft-designs of different WABs. The design is still not fixed! However, an already quite developed design of a WAB (we will call it here short-WAB) will be our relating point. The short-WAB has a length of 300 mm (?) with a ray barrier (basically, a doughnut-shaped disk) 200 mm away from the mirror-surface.
There are two other types of WAB: a moderate-WAB and an extreme-WAB. Each are featuring with different lengths (400 mm and 546 mm), while the ray barrier is at the end of each baffle.

Cryostat interior

The interior of the cryostat can be divided into three main parts regarding their seismic motion: the recoil mass, the assembly frame, and the inner shield of the cryostat. The recoil mass (made of polished titanium) is suspended with a Type-A suspension (in KAGRA terms) which means that the seismic motion coming from the ground is suppressed by several orders of magnitude in the frequency observation-range (10 – 100 Hz). A baffling of the recoil mass, thus, seems not be necessary. Yet, I will present the results of the simulations for completeness.

The assembly frame (made mainly of aluminum) is not suspended and will show characteristic eigenmodes. **However, the vibration spectrum has not yet been taken**. It lies in the main target range of light scattered light at wide and medium angles.

The inner shield of the cryostat is made of polished DLC and is thus shiny. This inner shield is mainly important for the back-scattering of short-angle scattered light, which means the surface area around the opening of the inner shield for the main beam is a target for scattering from the mirror.

Simulation results

The simulations have been done with “LightTools” as mentioned above. The number of rays that were produced by the model’s light-source has been set to 100 million constantly for all runs. To simulate the influence of different materials on the scattering, I used OPR-files, offered to us by different companies which take measurements on the reflection of these materials, where the scattering is thought to follow a Gaussian-like distribution.
The overall scattered light from the mirror is set to 1 W so that the incoming back-scattered power is always related to 1. The results for the different cases are summarized in Table 1.

	Recoil-mass	**Assembly frame**	**Inner shield**
without WAB	0.000538	0.000862	0.00206
short-WAB	“	0.000049	0.000268
moderate-WAB	“		
extreme-WAB	“	$3 \cdot 10^{-7}$	10^{-10}

Table 1: Results of the incident back-scattered power on the surface of the mirror in Watts. The numbers are related to 1 W total scattered power of the mirror.

In Figure 3-8 the intensity of the incoming back-scattered power is shown for all cases without any baffle. Thereby, both the areal and the angular distribution are shown for back-scattering from the recoil mass, the assembly frame, and the inner shield. It is obvious that the areal distribution of the intensity on the mirror is almost homogeneous for all three cases. Except the back-scattering from the assembly frame shows a slight decreasing of the intensity toward the edges of the mirror-surface.
However, a totally different view is shown by the angular distribution. As can be seen, it differs a lot for each case. While the recoil mass gives a relatively homogeneous angular distribution with an increasing intensity toward wider angles, the assembly frame and the inner shield have a highly inhomogeneous angular distribution due to the placement of the interior of the cryostat.

It is obvious that a WAB will have an enormous effect on the back-scattered power toward the mirror. But, the power alone is not important for the effect on the gravitational-wave strain. The phase noise of the light is even more important (see above equations). However, phase noise is different for each back-scattering surface. While the recoil mass is suspended like the mirror, assembly frame and inner shield are not. Moreover, it is likely that their motion is not only driven by the seismic motion of the KAGRA mine but also by the cryocooler that runs the cryostat.
Right now (03.2017), there are only data for the motion of the inner shield with cryocoolers on and off, respectively!

If we are putting the results of the simulations into a graph (Figure 9) showing the influence of the back-scattered light from each part on the sensitivity of KAGRA, we see that by far the most influence is coming from the inner shield, followed by the assembly frame and the recoil-mass. Thereby, I assumed (because of the lack of data) the motion of the assembly frame to be same as the

seismic

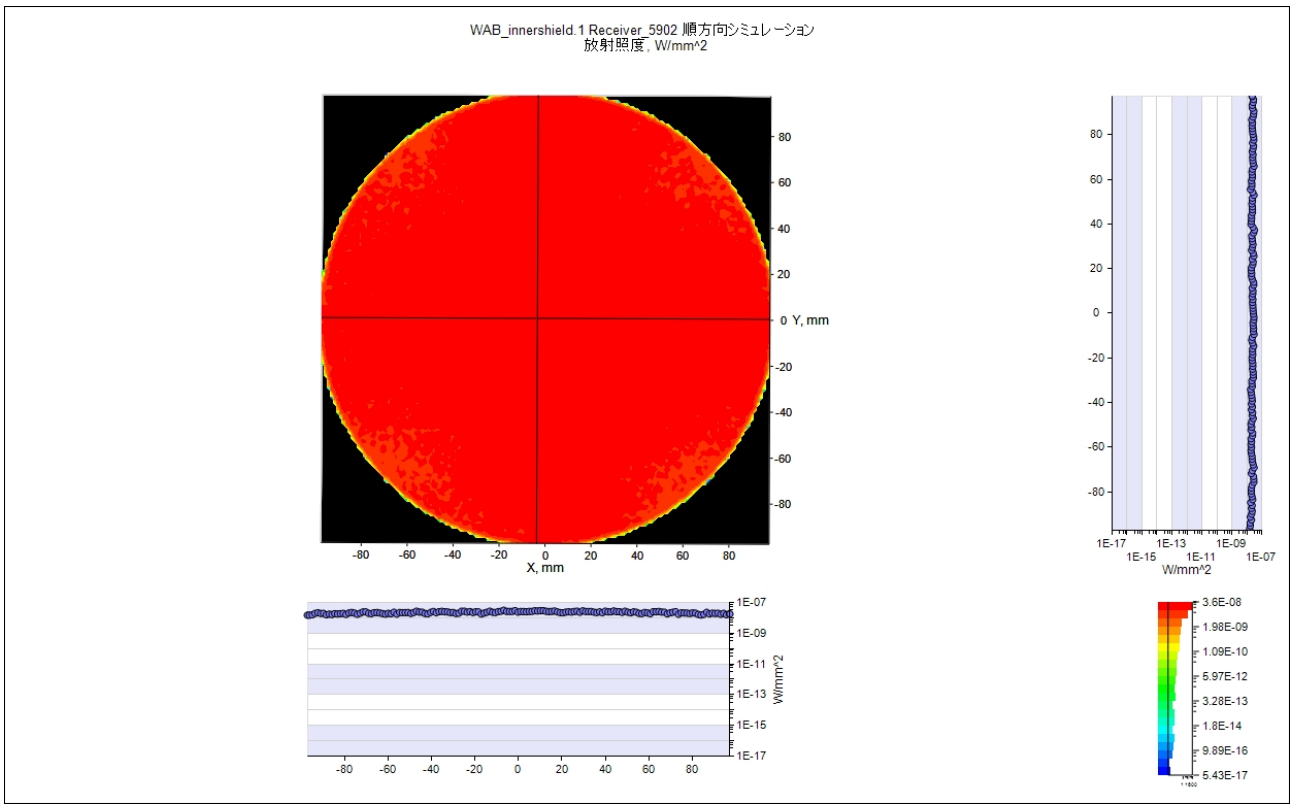

Figure 3: Map, showing the (non-baffled) intensity of the back-scattered light incident on the mirror from the recoil mass.

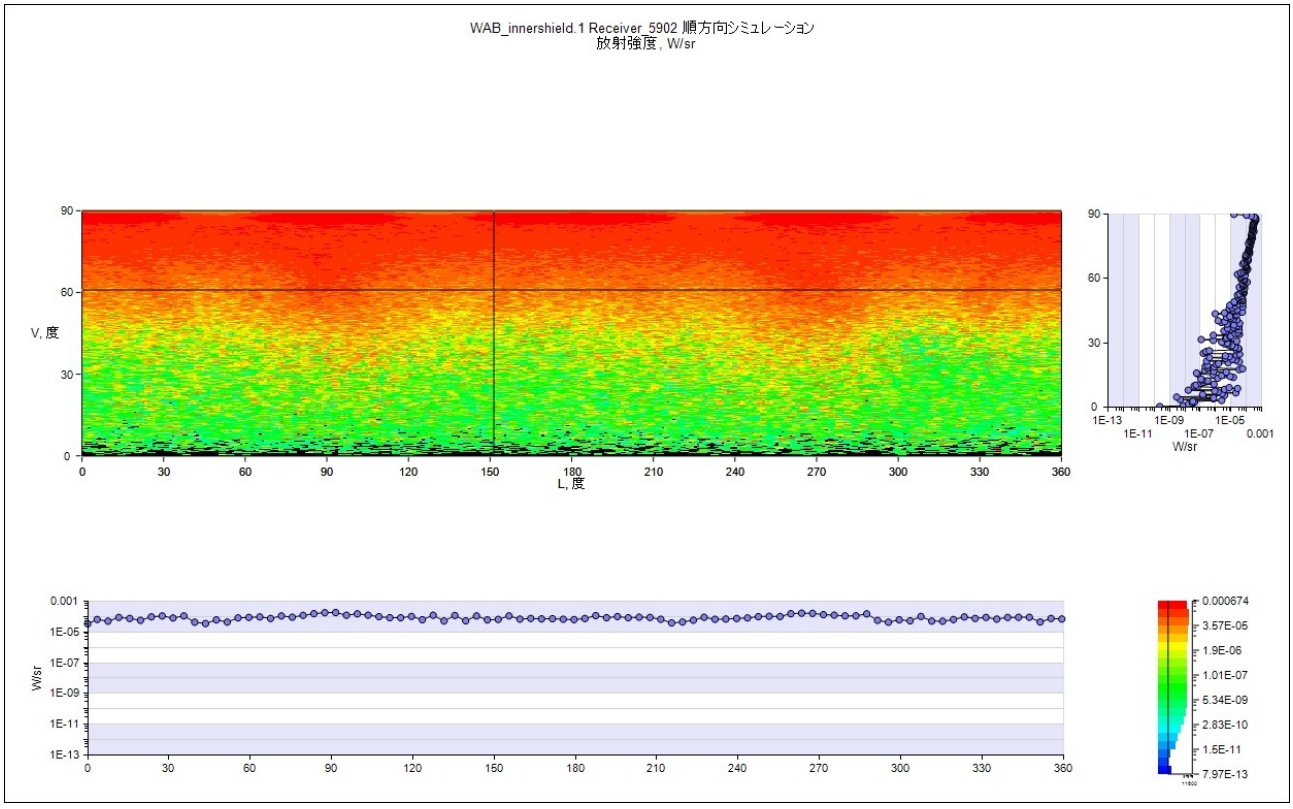

Figure 4: Angular distribution of the incoming intensity of the (non-baffled) back-scattered light incident on the mirror from the recoil mass.

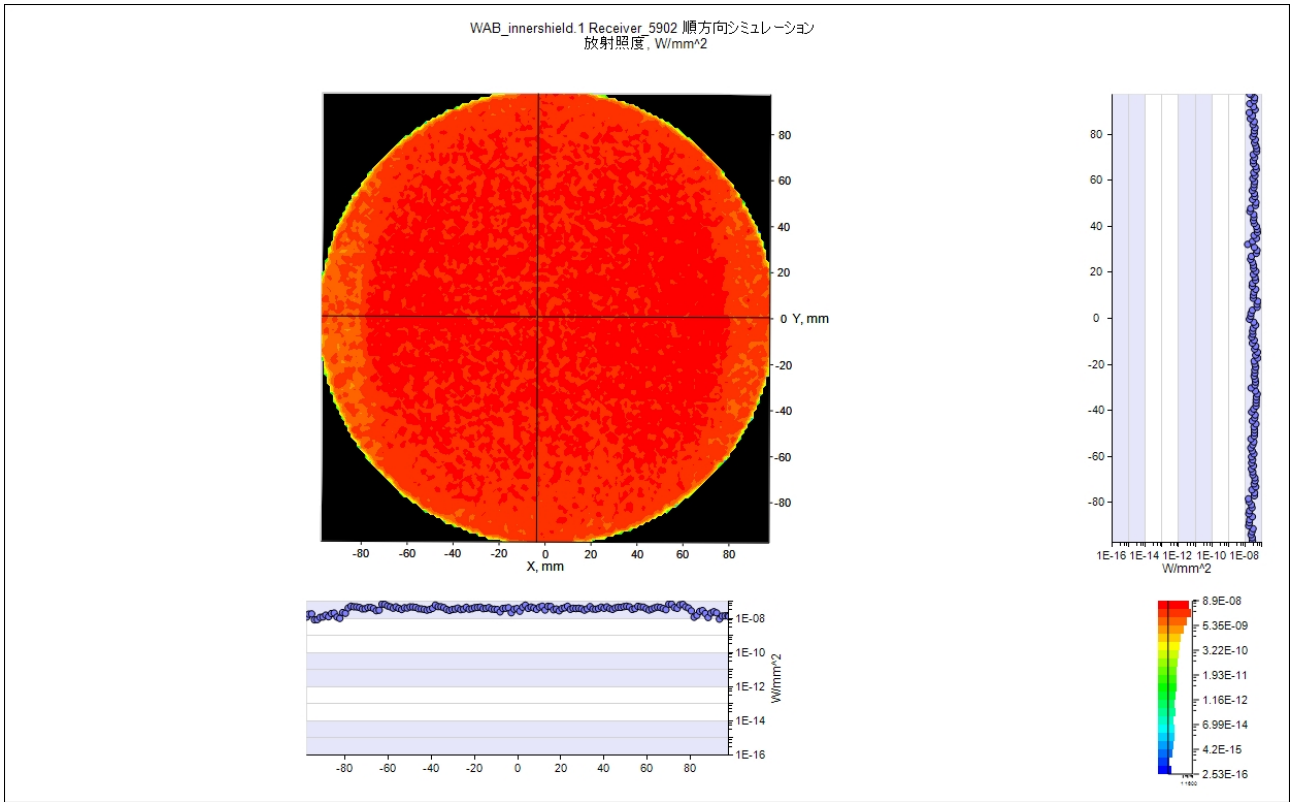

Figure 5: Map, showing the (non-baffled) intensity of the back-scattered light incident on the mirror from the assembly frame.

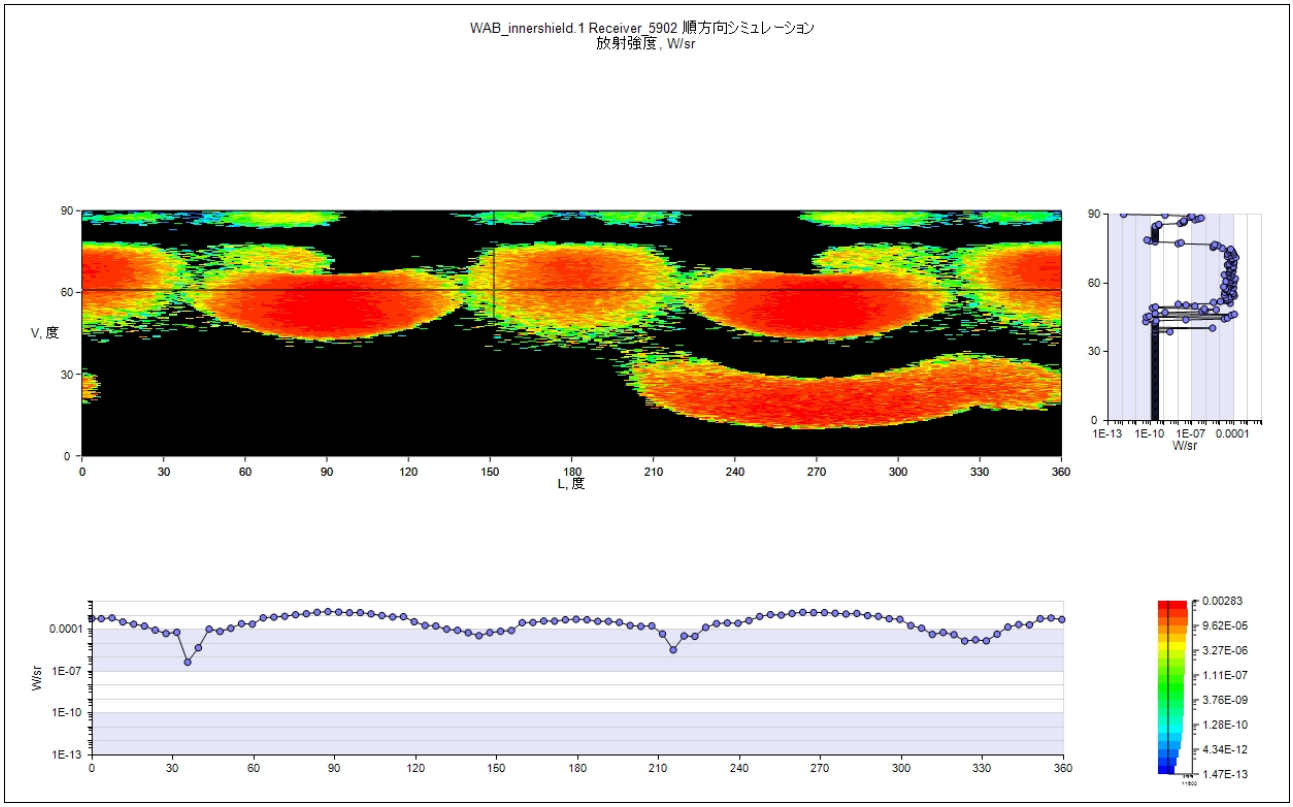

Figure 6: Angular distribution of the incoming intensity of the (non-baffled) back-scattered light incident on the mirror from the assembly frame.

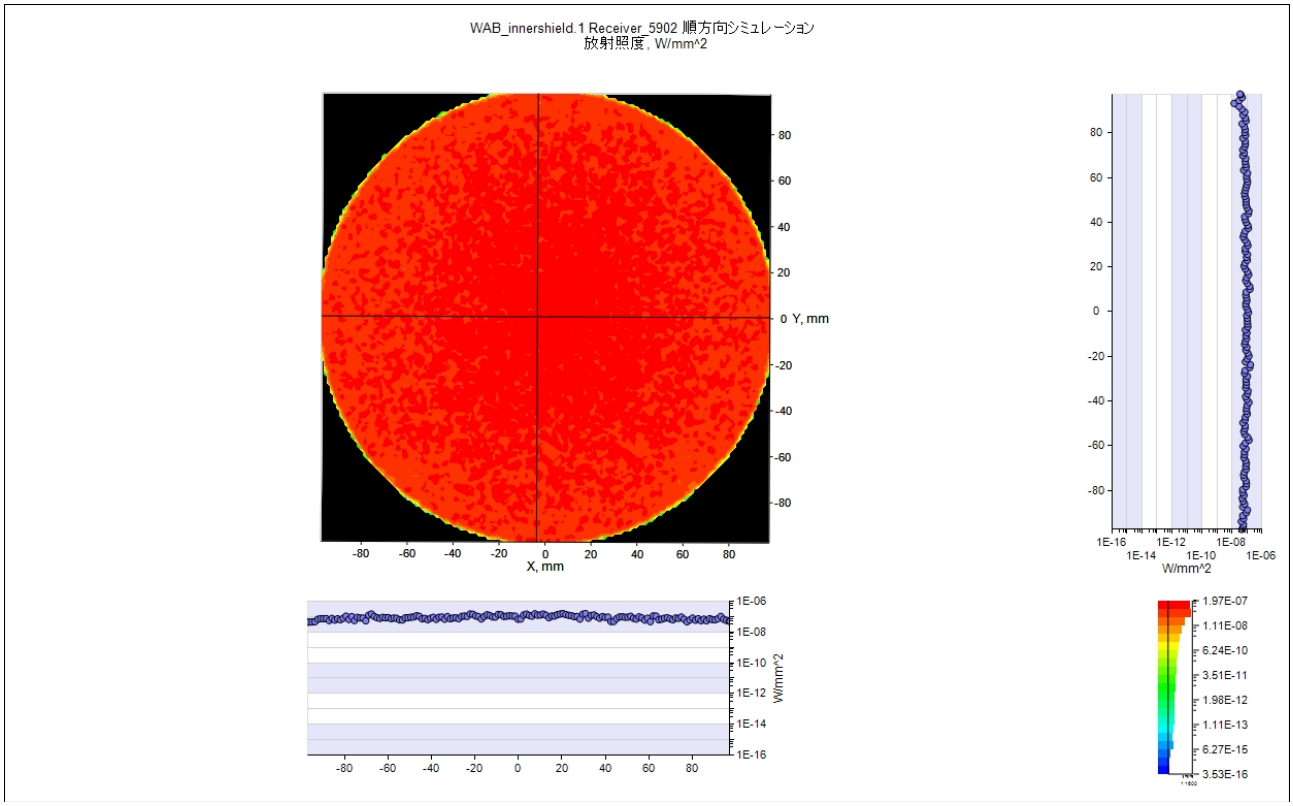

Figure 7: Map, showing the (non-baffled) intensity of the back-scattered light incident on the mirror from the inner shield.

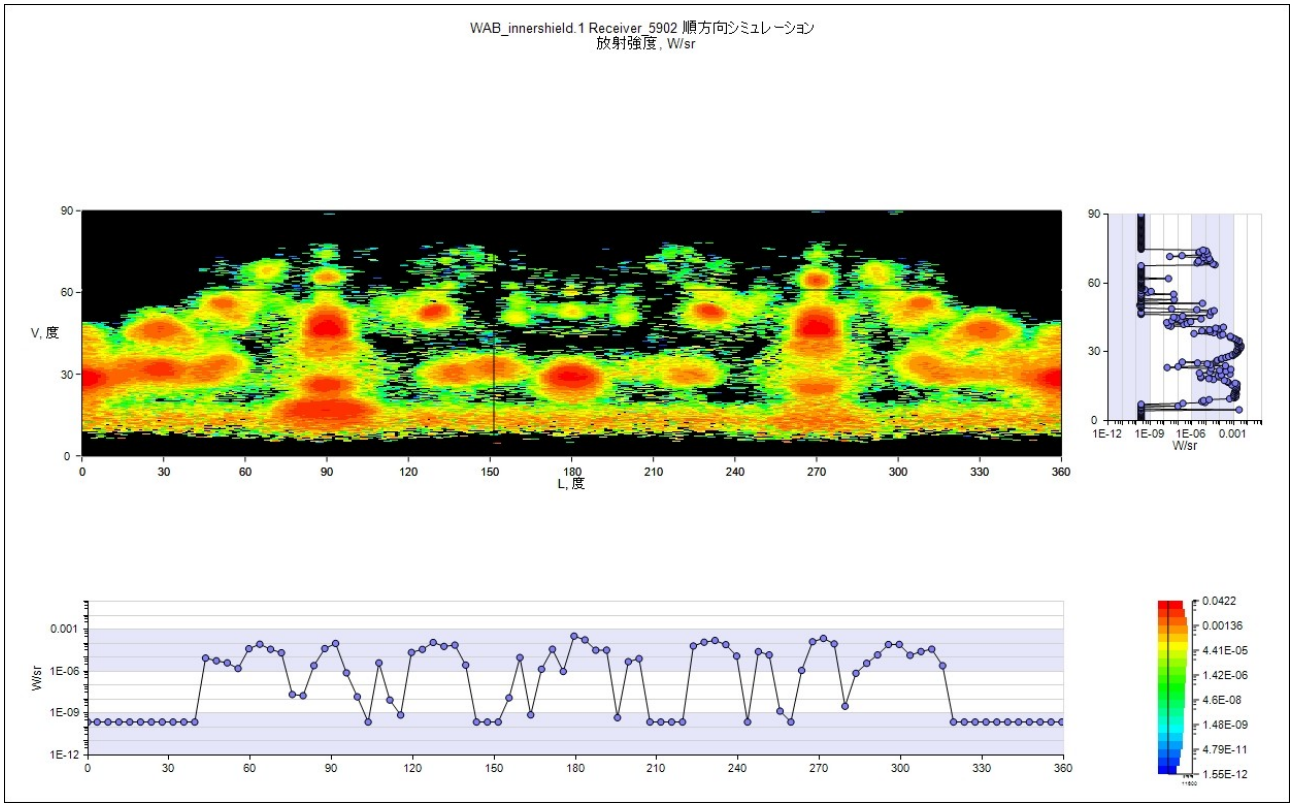

Figure 8: Angular distribution of the incoming intensity of the (non-baffled) back-scattered light incident on the mirror from the inner shield.

motion of the KAGRA ground.

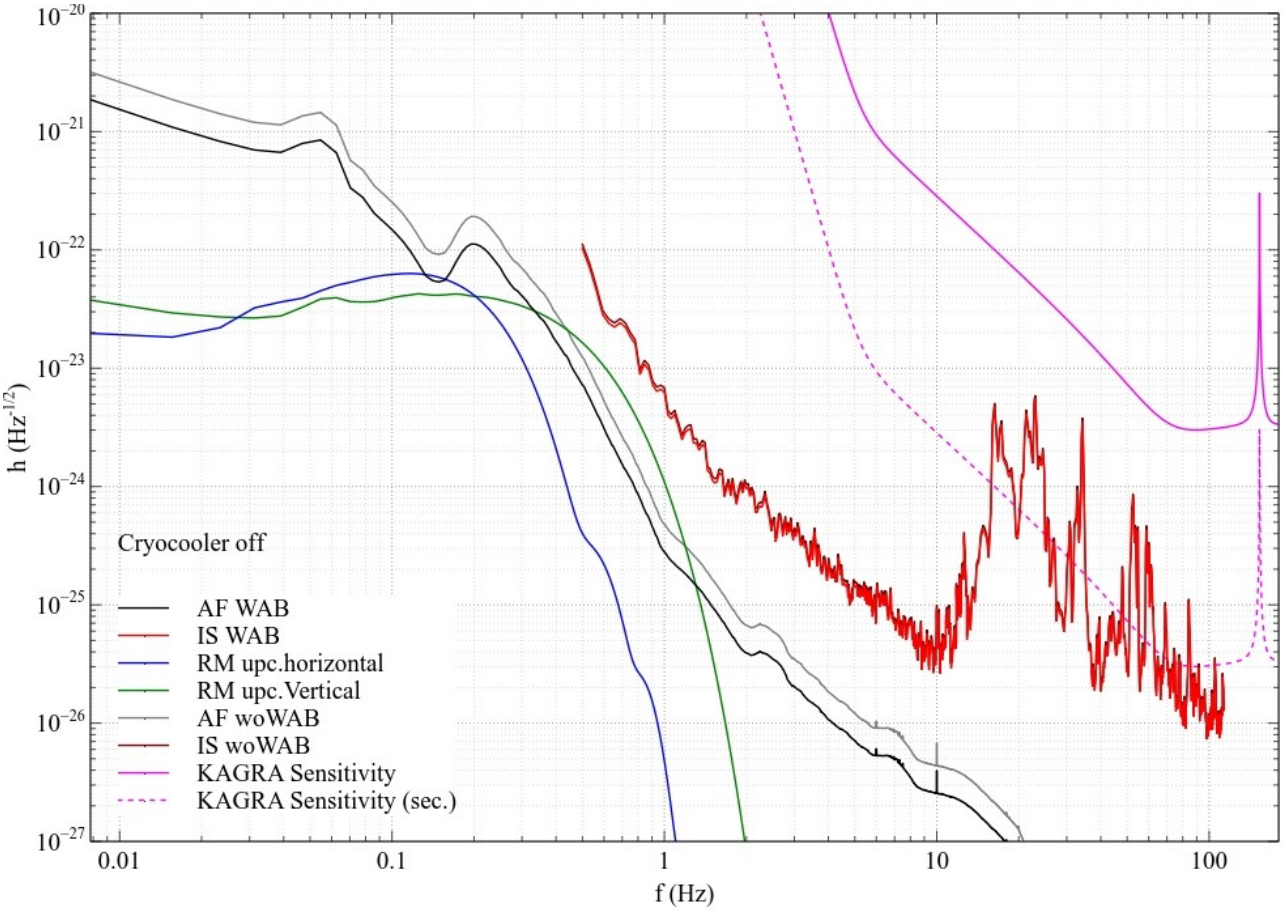

Figure 9: Strain-noise contribution of each component when cryocoolers are off (preliminary).

As can be seen, because of the characteristics of the vibrational noise of the inner shield, between 10 and 100 Hz the security threshold for KAGRA's sensitivity (1/100 of the actual sensitivity-goal) is violated for several peaks in the noise spectrum. The other contributions stay below the noise of the inner shield in the whole spectral area (**preliminary**).

In Figure 10 the spectral noise of the inner shield when the cryocooler is on is given in comparison with KAGRA's goal sensitivity and the security-sensitivity. Here, even the goal sensitivity is harmed for two peaks at around 35 and 110 Hz while the security-sensitivity region is broken for the whole spectral region between 15 and 120 Hz.

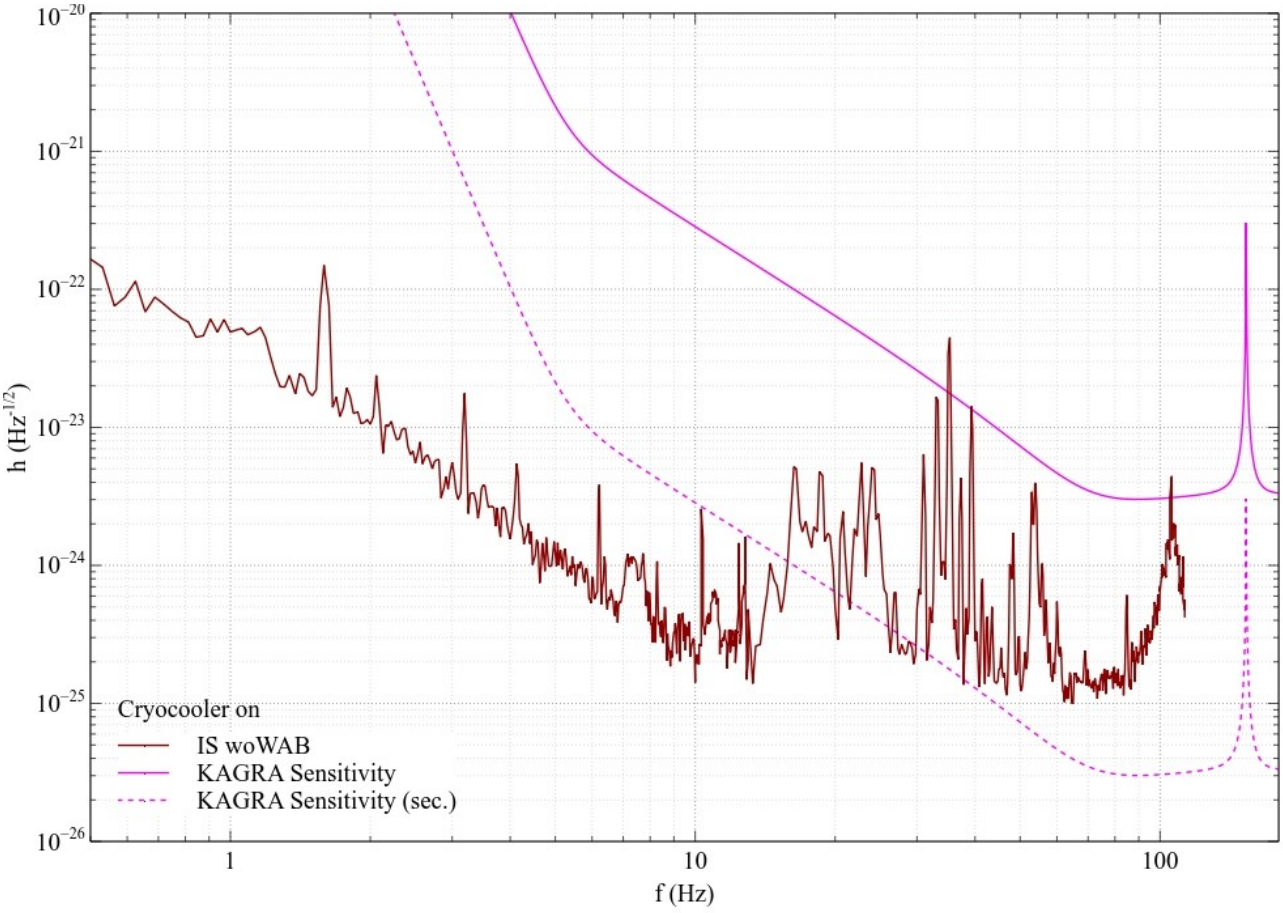

Figure 10: Strain noise of the inner shield when the cryocooler is on.